Int. J. Electrochem. Sci., 11 **(2016)** 4611 – 4618, doi: 10.20964/2016.06.14

International Journal of ELECTROCHEMICAL SCIENCE
www.electrochemsci.org

Short Communication

Structural and Properties of $LiNi_{0.5}Mn_{1.5}O_{4-\delta}$ and $LiNi_{0.5}Mn_{1.5}O_4$ Spinels: A first-Principles Investigation

Xinghua Liang[1*], *Meihong Huang*[1], *Yuchao Zhao*[1], *Hanjie Wu*[1], *Yujiang Wang*[2], *Fawei Tang*[3]

[1] Guangxi Key Laboratory of Automobile Components and Vehicle Technology, Guangxi University of Science and Technology, Liuzhou 545006, China.
[2] College of Mechanical Engineering, Guangxi University, Nanning 530004, China.
[3] College of Material Science and Engineering, Beijing university of Technology, Beijing 100124, China.
[*]E-mail: LXH304@aliyun.com

Received: 28 October 2015 / *Accepted:* 15 December 2015 / *Published:* 4 May 2016

The structural and properties of $LiNi_{0.5}Mn_{1.5}O_4$-*Fd-3m* and $LiNi_{0.5}Mn_{1.5}O_4$-$P4_332$ spinels as the high-voltage cathode materials were investigated by the first-principles theory. The calculated results indicate that the crystal structure of the $LiNi_{0.5}Mn_{1.5}O_4$-*Fd-3m* is beneficial to the transition of lithium compared with $LiNi_{0.5}Mn_{1.5}O_4$-$P4_332$. Due to the charge overlap of $LiNi_{0.5}Mn_{1.5}O_4$-$P4_332$ around Mn, Ni and O atoms significantly increased compared with $LiNi_{0.5}Mn_{1.5}O_4$-*Fd-3m*, which form a stable bond, therefore their structure is significantly increased. The lengths of the bonds of $LiNi_{0.5}Mn_{1.5}O_4$-$P4_332$ are shorter than that of the $LiNi_{0.5}Mn_{1.5}O_4$-*Fd-3m*, indicating that the energy of the bond is smaller, thus the structure of $LiNi_{0.5}Mn_{1.5}O_4$-$P4_332$ is more stable, but the Mn-Mn bonds hinder the shuttle movement of lithium ions, so the cycle performance of $LiNi_{0.5}Mn_{1.5}O_4$-*Fd-3m* may be better than that of $LiNi_{0.5}Mn_{1.5}O_4$-$P4_332$. The calculated results exhibit the band gap of $LiNi_{0.5}Mn_{1.5}O_4$-*Fd-3m* and $LiNi_{0.5}Mn_{1.5}O_4$-$P4_332$ are 0.487 eV and 0.718 eV, respectively， which indicate that the eletro-conductive performance $LiNi_{0.5}Mn_{1.5}O_4$-*Fd-3m* is better.

Keywords: first-principles, electrochemical performance, structure, spinel $LiNi_{0.5}Mn_{1.5}O_4$

1. INTRODUCTION

With many advantages such as no memory effect, the best energy-to-weight ratios, and a slow loss of charge when not in use, Lithium-ion batteries have been favored in consumer electronics for last 30 years [1,2]. It has been well known that some important factors such as the types of electrolyte used, and the nature of cathode and anode, have great impact on the battery property [3-7]. Compared with other cathode materials, the charge/discharge voltage platform of $LiNi_{0.5}Mn_{1.5}O_4$ spinel material is about 4.7 V, thereby it was a worthwhile study cathode material for new-generation lithium-ion batteries [8,9]. Because of the synthetic temperature, atmospheric conditions and other factors, $LiNi_{0.5}Mn_{1.5}O_4$ has two different crystal structures, they are $P4_332$ and *Fd-3m* structure [10]. Stoichiometric $LiNi_{0.5}Mn_{1.5}O_4$ has a cubic, primitive structure ($P4_332$), while nonstoichiometric $LiNi_{0.5}Mn_{1.5}O_{4-\delta}$ has a normal face-centered spinel structure(*Fd-3m*). For $LiNi_{0.5}Mn_{1.5}O_4$, only part of manganese atoms in 16d position is occupied by nickel atoms randomly, while for $LiNi_{0.5}Mn_{1.5}O_{4-\delta}$, manganese atoms in 4a position were occupied by nickel atoms orderly [11-13]. This paper study mainly on the difference of crystal structure, density of states, bond length, atomic layout and charge density between $LiNi_{0.5}Mn_{1.5}O_4$ and $LiNi_{0.5}Mn_{1.5}O_{4-\delta}$ spinels by means of first-principles theory. Meanwhile, we discussed the impact of these properties on their electrochemical properties such as structural stability and electronic conductivity.

2. METHODS

Computations in this study were performed with CASTEP code (Materials Studio package) within the generalized gradient approximation (GGA) and following structural models [14]. Li-2s, O-2s2p, Ni-3d4s, Mn-3d4s electrons are chosen as valence electrons, while all the other electrons are chosen as core electrons. The ionic positions and the lattice parameters were fully relaxed before the calculations, and the final force on each atom is less than 0.02 eV/A. A plane-waves cut-off energy of 300 eV and 2×2×2 Monk horst–Pack k-point over the irreducible Brillouin zone were applied in the calculations [15]. Gaussian smearing method with a smearing width of 0.03 eV was chosen in the calculation of the density of states (DOS). Conventional cell was chosen in the calculations. Here, $LiNi_{0.5}Mn_{1.5}O_4$ and $LiNi_{0.5}Mn_{1.5}O_{4-\delta}$ are referred to as $LiNi_{0.5}Mn_{1.5}O_4$-$P4_332$ and $LiNi_{0.5}Mn_{1.5}O_4$-*Fd-3m*, respectively. In this paper, we mainly analyzed the crystal structure, density of states, bond length, atomic layout and charge density of $LiNi_{0.5}Mn_{1.5}O_4$-$P4_332$ and $LiNi_{0.5}Mn_{1.5}O_4$-*Fd-3m*. $LiNi_{0.5}Mn_{1.5}O_4$-$P4_332$ and $LiNi_{0.5}Mn_{1.5}O_4$-*Fd-3m* were prepared by sol gel method as the anode material of battery.

3. RESULTS AND DISCUSSION

3.1 Structures of $LiNi_{0.5}Mn_{1.5}O_4$-Fd-3m and $LiNi_{0.5}Mn_{1.5}O_4$-$P4_332$

The calculation model was given in Fig. 1. For $LiNi_{0.5}Mn_{1.5}O_4$-*Fd-3m* (Fig. 1a), 8a sites are located by Li ions, 16d sites are occupied by Mn and Ni ions and distributed in 32e sites are O ions, which consisting of a normal face-centered spinel array, while for $LiNi_{0.5}Mn_{1.5}O_4$-$P4_332$ (Fig. 1b), 8c sites are located by Li ions, 12d sites and 4a sites are occupied by Mn ions and Ni ions respectively, and distributed in 8c and 24e sites are O ions, which consisting of a primitive, or simple, cubic array. It is consistent with the resultls in Refs. [16], [17] and [18]. The lattice parameters [19] for *$LiNi_{0.5}Mn_{1.5}O_4$-Fd-3m and $LiNi_{0.5}Mn_{1.5}O_4$-$P4_332$* are 8.166 Å and 8.172 Å. Thence, the fundamental difference is where Ni ions are located. It is well known that the crystal structure of $LiNi_{0.5}Mn_{1.5}O_4$-

Fd-3m is benefit to the transition of lithium comparing with $LiNi_{0.5}Mn_{1.5}O_4$-*$P4_332$*. The Mn-Mn bonds of $LiNi_{0.5}Mn_{1.5}O_4$-*$P4_332$* make the crystal framework more stable, but which hinder the shuttle movement of lithium ions. It is show evidence of stability of crystal structure in charge-discharge recycling process, which is consistent with the experimental resultls in Fig. 2.

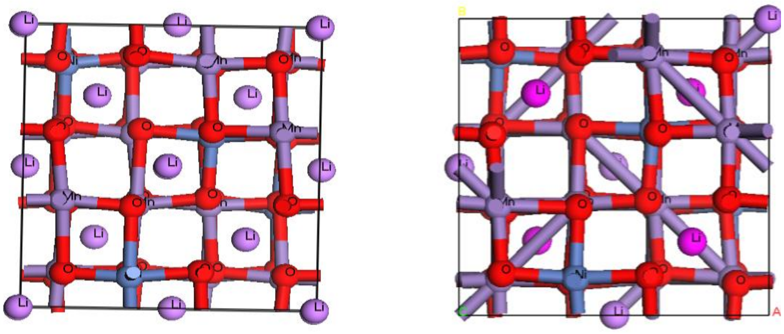

(a) (b)

Figure 1. Structure cell chart of (a) $LiNi_{0.5}Mn_{1.5}O_4$-*Fd-3m* (b) $LiNi_{0.5}Mn_{1.5}O_4$-*$P4_332$*.

3.2 Charge-discharge performance

The first charge-discharge curves and the cycle performances of $LiNi_{0.5}Mn_{1.5}O_4$-*Fd-3m* and $LiNi_{0.5}Mn_{1.5}O_4$-*$P4_332$* at 0.1 C are shown in Fig. 2. The cut-off voltages were 3.5-4.8 V at room temperature. Fig.2a showed that the charge and discharge specific capacity of the $LiNi_{0.5}Mn_{1.5}O_4$-*Fd-3m* was 119.45 $mAhg^{-1}$, 112.44 $mAhg^{-1}$ respectively, while the charge and discharge specific capacity of the $LiNi_{0.5}Mn_{1.5}O_4$-*$P4_332$* was 100.26 $mAhg^{-1}$, 90.23 $mAhg^{-1}$ respectively. It can be found from Fig. 2b that the cycle property of the $LiNi_{0.5}Mn_{1.5}O_4$-*Fd-3m* also better than the $LiNi_{0.5}Mn_{1.5}O_4$-*$P4_332$*, which is consistent with the calculational resultls in Fig. 1.

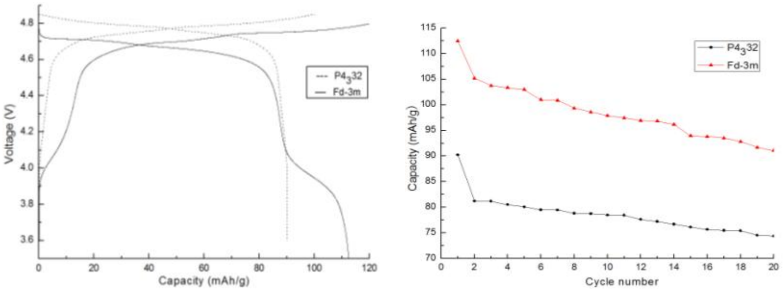

(a) (b)

Figure 2. (a) First charge-discharge (b) Cycle performances of $LiNi_{0.5}Mn_{1.5}O_4$-*Fd-3m* and $LiNi_{0.5}Mn_{1.5}O_4$-*$P4_332$*.

3.3 Density of states

The electron density of states (DOS) and projected electron density of states (PDOS) of $LiNi_{0.5}Mn_{1.5}O_4$-*Fd-3m* and $LiNi_{0.5}Mn_{1.5}O_4$-$P4_332$ are shown in Fig. 3, respectively. From the figure, it can be found that the DOS mainly attributed to s, p and d orbits. The calculated band gap of $LiNi_{0.5}Mn_{1.5}O_4$-*Fd-3m* and $LiNi_{0.5}Mn_{1.5}O_4$- $P4_332$ is 0.487 eV and 0.718 eV, respectively. The band gap of the $LiNi_{0.5}Mn_{1.5}O_4$-*Fd-3m* is smaller than that of the $LiNi_{0.5}Mn_{1.5}O_4$-$P4_332$, thereby the free electrons transitional energy of the $LiNi_{0.5}Mn_{1.5}O_4$-*Fd-3m* are less than that of the $LiNi_{0.5}Mn_{1.5}O_4$-$P4_332$, which suggests that the $LiNi_{0.5}Mn_{1.5}O_4$-*Fd-3m* may exhibit higher electronic conduction compared with $LiNi_{0.5}Mn_{1.5}O_4$-$P4_332$. The PDOS of different chemical elements of $LiNi_{0.5}Mn_{1.5}O_4$-*Fd-3m* and $LiNi_{0.5}Mn_{1.5}O_4$-$P4_332$ are shown in Fig 4. For the $LiNi_{0.5}Mn_{1.5}O_4$-$P4_332$, the energy provided by O, Mn and Ni was higher than that of the $LiNi_{0.5}Mn_{1.5}O_4$-*Fd-3m*. This may be the reason why the space frame of the $LiNi_{0.5}Mn_{1.5}O_4$-*Fd-3m* is more stable compared with $LiNi_{0.5}Mn_{1.5}O_4$-$P4_332$, which is consistent with the charge-discharge and cycling curves in Fig. 2.

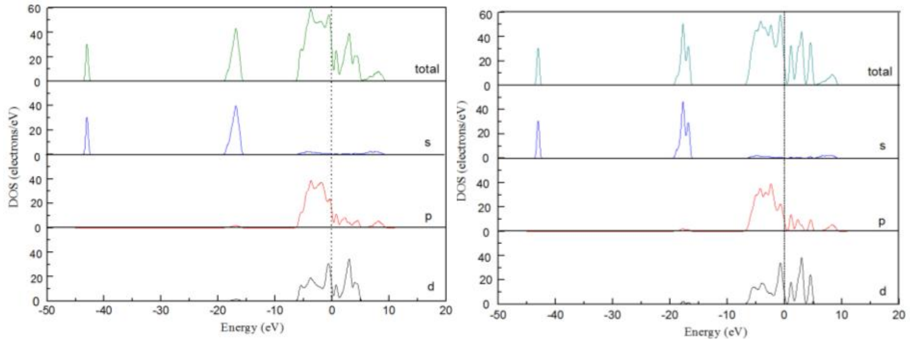

(a) (b)

Figure 3. The density of states of (a) $LiNi_{0.5}Mn_{1.5}O_4$-*Fd-3m* (b) $LiNi_{0.5}Mn_{1.5}O_4$-$P4_332$. The Fermi level is set to be zero.

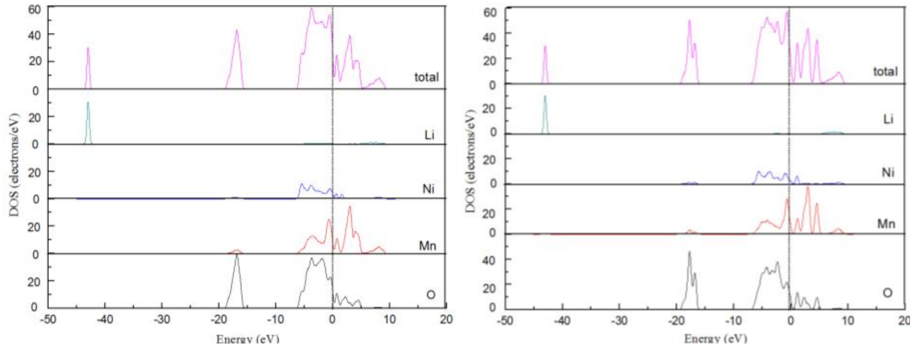

(a) (b)

Figure 4. The different chemical elements density of states of (a) $LiNi_{0.5}Mn_{1.5}O_4$-*Fd-3m* (b) $LiNi_{0.5}Mn_{1.5}O_4$-$P4_332$.

To further analyze the impact of different chemical elements on the DOS of the $LiNi_{0.5}Mn_{1.5}O_4$-*Fd-3m and* $LiNi_{0.5}Mn_{1.5}O_4$-$P4_332$, we have plotted the orbit of different chemical elements, which are shown in Fig. 5. The energy distribution of Li of the $LiNi_{0.5}Mn_{1.5}O_4$-$P4_332$ is wider compared with $LiNi_{0.5}Mn_{1.5}O_4$-*Fd-3m*, which suggests that for the $LiNi_{0.5}Mn_{1.5}O_4$-$P4_332$, Li suffers from more binding force, therefore the number of free ions are relatively small. This may be the reason why the capacity of the $LiNi_{0.5}Mn_{1.5}O_4$-$P4_332$ is less than the $LiNi_{0.5}Mn_{1.5}O_4$-*Fd-3m*. From Figs. 5b and c, it is interesting to see that for the $LiNi_{0.5}Mn_{1.5}O_4$-*Fd-3m*, the concentrations of energy distribution of Ni is increased, which cause better electronic conductivity compared with $LiNi_{0.5}Mn_{1.5}O_4$-$P4_332$. At the right of Fermi level, the energy of the $LiNi_{0.5}Mn_{1.5}O_4$-$P4_332$ is wider and sharper, which imply the Ni-O bond is more stable, thus the cycle stability is better.

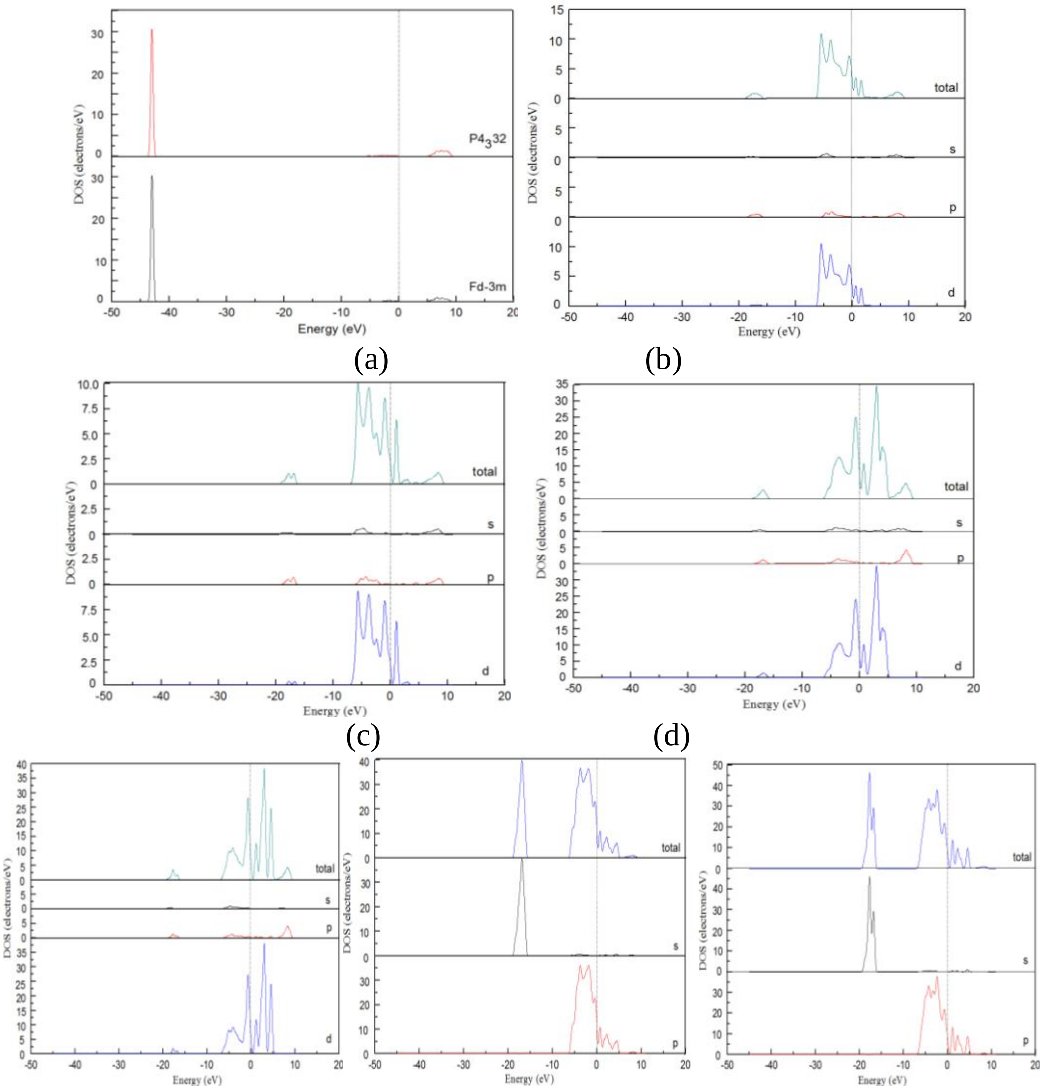

(a) (b)

(c) (d)

(e) (f) (g)

Figure 5. (a) Li density of states. Ni density of states of (b) $LiNi_{0.5}Mn_{1.5}O_4$-*Fd-3m* and (c) $LiNi_{0.5}Mn_{1.5}O_4$-$P4_332$. Mn density of states of (d) $LiNi_{0.5}Mn_{1.5}O_4$-*Fd-3m* and (e) $LiNi_{0.5}Mn_{1.5}O_4$-$P4_332$. O density of states of (f) $LiNi_{0.5}Mn_{1.5}O_4$-*Fd-3m* and (g) $LiNi_{0.5}Mn_{1.5}O_4$-$P4_332$.

Taking all above diagrams into consideration, we can get the following conclusions. Energy distribution in the range of -10 ~ 5eV is mainly Ni-O, Mn-O bonds with strong force, which formed through electrons overlap of O-2p, Ni-3d and Mn-3d. The comparison between the intensity degree of Li of $LiNi_{0.5}Mn_{1.5}O_4$-$P4_332$ and $LiNi_{0.5}Mn_{1.5}O_4$-*Fd-3m* reveals that for $LiNi_{0.5}Mn_{1.5}O_4$-$P4_332$ the impact of other orbitals on Li^+ is larger, thereby it is easy to cause the decrease of the capacity of lithium ion batteries.

3.4 Atomic and bond layout analysis

Table 1. The atomic layout of the $LiNi_{0.5}Mn_{1.5}O_4$-*Fd-3m* (e)

atom	s	p	d	total charge	net charge
Li	2.00	0.00	0.00	2.00	1.00
Ni	0.46	0.66	8.12	9.23	0.77
Mn	0.35	0.45	5.29	6.08	0.92
O	1.90	4.79	0.00	6.69	-0.69

Table 2. The atomic layout of the $LiNi_{0.5}Mn_{1.5}O_4$-$P4_332$ (e)

atom	s	p	d	total charge	net charge
Li	1.97	0.00	0.00	1.97	1.03
Ni	0.46	0.70	8.12	9.27	0.73
Mn	0.32	0.43	5.34	6.09	0.91
O	1.89	4.80	0.00	6.69	-0.69

Table 3. The bond length and bond layout of $LiNi_{0.5}Mn_{1.5}O_4$-*Fd-3m and* $LiNi_{0.5}Mn_{1.5}O_4$-$P4_332$

		Li-O	Ni-O	Mn-O
bond length (Å)	$LiNi_{0.5}Mn_{1.5}O_4$ -*Fd-3m*	2.015	2.025	2.101
	$LiNi_{0.5}Mn_{1.5}O_4$ -$P4_332$	1.956	1.981	2.065
bond layout (e)	$LiNi_{0.5}Mn_{1.5}O_4$ -*Fd-3m*	0.022	0.305	0.263
	$LiNi_{0.5}Mn_{1.5}O_4$ -$P4_332$	0.001	0.32	0.235

For the $LiNi_{0.5}Mn_{1.5}O_4$-*Fd-3m*, the total charge and net charge of Li atoms and the theoretical value are almost identical, which indicate that the ionization degree of Li atoms are higher than that of the $LiNi_{0.5}Mn_{1.5}O_4$-$P4_332$, thereby it is easy lead to electrons lost and turn into plasma state. This may be the reason why the charge and discharge capacity of the $LiNi_{0.5}Mn_{1.5}O_4$-*Fd-3m* is larger than that of the $LiNi_{0.5}Mn_{1.5}O_4$-$P4_332$. The net charge of the $LiNi_{0.5}Mn_{1.5}O_4$-$P4_332$ is different from the theoretical net charge, which shows that the ionic and covalent of Ni and Mn of the $LiNi_{0.5}Mn_{1.5}O_4$-$P4_332$ are relatively strong, thereby it is easy to form Ni-O, Mn-O, and Mn-Mn bonds with atoms surrounding.

The lengths of the Ni-O and Mn-O bonds of the $LiNi_{0.5}Mn_{1.5}O_4$-*Fd-3m* are longer than that of the $LiNi_{0.5}Mn_{1.5}O_4$-$P4_332$, the difference is 0.044 Å and 0.036 Å, respectively, which demonstrate that the covalent of Ni-O and Mn-O bonds of the $LiNi_{0.5}Mn_{1.5}O_4$-$P4_332$ with a stable skeleton is stronger and more stable. The stability of the $LiNi_{0.5}Mn_{1.5}O_4$-*Fd-3m* is not as good as the $LiNi_{0.5}Mn_{1.5}O_4$-$P4_332$, and easy to occur lattice collapse and cause Jahn-Tener effect in charging and discharging process, which behaves as the declining of capacity and the deteriorated of cycling performance. The lengths of the Li-O bonds of the $LiNi_{0.5}Mn_{1.5}O_4$-*Fd-3m* are longer than that of the $LiNi_{0.5}Mn_{1.5}O_4$-$P4_332$, which reveals that Li-O bonds of the $LiNi_{0.5}Mn_{1.5}O_4$-*Fd-3m* is quite weak, and the diffusion coefficient of lithium ion is comparatively large and more capacity.

3.5 Analysis of difference of charge density

The charge density of $LiNi_{0.5}Mn_{1.5}O_4$-*Fd-3m* and $LiNi_{0.5}Mn_{1.5}O_4$-$P4_332$ are shown in Fig. 6. It is interesting to see that for $LiNi_{0.5}Mn_{1.5}O_4$-$P4_332$, the charge overlap around Mn, Ni and O atoms significantly increased compared with $LiNi_{0.5}Mn_{1.5}O_4$-*Fd-3m*. Meanwhile, it can be found that the charge of Ni, Mn and O atoms formed Ni-O and Mn-O stable bonds, therefore $LiNi_{0.5}Mn_{1.5}O_4$-$P4_332$ structural stability is dramatically increased compared with $LiNi_{0.5}Mn_{1.5}O_4$-*Fd-3m*. For $LiNi_{0.5}Mn_{1.5}O_4$-*Fd-3m*, the charge density among Ni， Mn and O atoms decreases simultaneously, so the partial charge from the Ni, Mn and O atoms is centralized near Li-site atoms. Therefore the electronic conductivity of $LiNi_{0.5}Mn_{1.5}O_4$-*Fd-3m* are improve enormously than that of the $LiNi_{0.5}Mn_{1.5}O_4$-$P4_332$, which reveals that $LiNi_{0.5}Mn_{1.5}O_4$-*Fd-3m* has better electronic properties and more capacity.

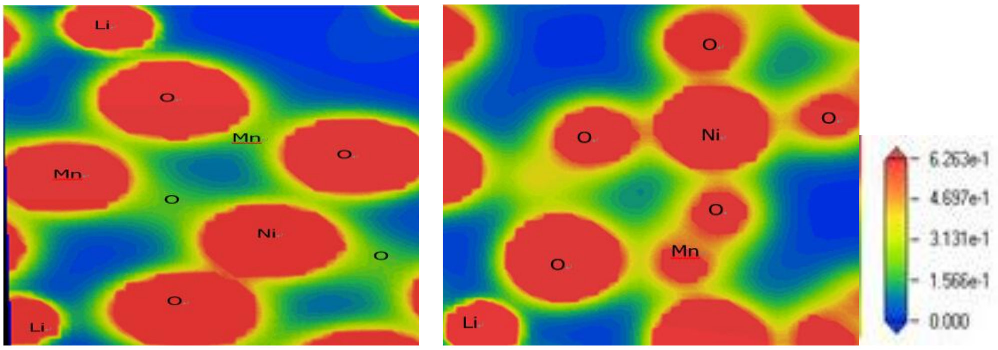

(a) (b)

Figure 6. Electric charge density difference of (a) $LiNi_{0.5}Mn_{1.5}O_4$-*Fd-3m* (b) $LiNi_{0.5}Mn_{1.5}O_4$-$P4_332$.

4. CONCLUSIONS

In conclusion, we have investigated Structural and properties of the $LiNi_{0.5}Mn_{1.5}O_4$-*Fd-3m and* $LiNi_{0.5}Mn_{1.5}O_4$-$P4_332$. The calculated results indicate that the crystal structure of the $LiNi_{0.5}Mn_{1.5}O_4$-*Fd-3m* is benefit to the transition of lithium compared with $LiNi_{0.5}Mn_{1.5}O_4$-$P4_332$. Due to the charge overlap of $LiNi_{0.5}Mn_{1.5}O_4$-$P4_332$ around Mn, Ni and O atoms significantly increased compared with $LiNi_{0.5}Mn_{1.5}O_4$-*Fd-3m*, which form a stable bond, therefore their structure is significantly increased. The lengths of the bonds of $LiNi_{0.5}Mn_{1.5}O_4$-$P4_332$ are shorter than that of the $LiNi_{0.5}Mn_{1.5}O_4$-*Fd-3m*, indicating that the energy of the bond is smaller, thus the structure of $LiNi_{0.5}Mn_{1.5}O_4$-$P4_332$ is more stable, but the Mn-Mn bonds hinder the shuttle movement of lithium ions, so the cycle performance of $LiNi_{0.5}Mn_{1.5}O_4$-*Fd-3m* may better than that of $LiNi_{0.5}Mn_{1.5}O_4$-$P4_332$.

ACKNOWLEDGEMENTS
This project was funded by the Building Fund (No.13-051-38) of Guangxi Key Laboratory of Automobile Components and Vehicle Technology. And it was financially supported by the innovation project of Guangxi Education (YCSZ2014201) and Guangxi Natural Science Fund (No. 2013GXNSFAA019317). We gratefully acknowledge support from Dr. Wang Yujiang and Dr. Tang Fawei in the computing.

References

1. Haisheng Fang, Zhixing Wang, *Mater. Res. Lett.* 60 (2006) 1273.
2. ChihYuan Lin, JenqGong Duh, Mater. Res. Lett. 64 (2010) 2328.
3. Ou Sha, Shaoliang Wang, Zhi Qiao, Wei Yuan, Zhiyuan Tang, *Mater. Res. Lett*., 89 (2012) 251.
4. Y.K. Yoon, C.W. Park, H.Y. Ahn, D.H. Kim, *J. Phys. Chem. Solids*., 68 (2007) 780.
5. Masanobu Nakayama, Masayuki Nogami, *Solid State Commun*., 150 (2010) 1329.
6. Huiming Wu, Ch. Venkateswara Rao, B. Rambabu, *Mater. Chem. Phys*., 116 (2009) 532.
7. N. Amdouni, K. Zaghib, F. Gendron, A. Mauger, *J. Magn. Magn. Mater*., 309 (2007) 100.
8. U. Lafont, C. Locati, W.J.H. Borghols, A. Łasin ska, J. Dygas, *J. Power Sources*, 189 (2009) 179.
9. Ippei Kishida, Kengo Orita, Atsutomo Nakamura, Yoshiyuki Yokogawa, *J. Power Sources*, 241 (2013) 1.
10. Bin Huang, Xinhai Li, Zhixing Wang, Huajun Guo, Xunhui Xiong, Jiexi Wang, J. *Alloys Compd*., 583 (2014) 313.
11. Hailong Wang, Hui Xia, Man On Lai, Li Lu, *Electrochem. Commun*., 11 (2009) 1539.
12. Jinyi Shi, Yuansheng Ding, *Shandong Chemical Industry*, 41 (2012) 18.
13. Masanobu Nakayama, Mayumi Kaneko, *Chem. Phys*., 14 (2012) 13963.
14. Bo Xu, Shirley Meng, *J. Power Sources*, 195 (2010) 4971.
15. L. Wang, T. Maxisch, and G. Ceder, *Chem. Mater*., 19 (2007) 543.
16. Xiaogui Xin, Jingqin Shen, and Siqi Shi. *Chin.Phys.B.*, 12 (2012) 128202.
17. M. Kunduraci and G. Amatucci, *J.Electrochem.Soc*., 153 (2006) 1345.
18. Ariyoshi K, Iwakoshi Y, Nakayama N and Ohzuku T, *J.Electrochem.Soc*., 151 (2004) 296.
19. Kim J H, Myung S T, Yoon C S and Kang S G, *Chem. Mater*.,16 (2004) 906.